Steel and Composite Structures, *Vol. 18, No. 2 (2015) 467-480*
DOI: http://dx.doi.org/10.12989/scs.2015.18.2.467

Mechanical characteristics of hollow shear connectors under direct shear force

Kojiro Uenaka [*1] and Hiroshi Higashiyama [2a]

[1] *Department of Civil Engineering, Kobe City College of Technology, Gakuenhigashimachi 8-3, Nishi, Kobe, 6512194, Japan*
[2] *Department of Civil and Environmental Engineering, Kinki University, Kowakae 3-4-1, Higashiosaka, 5778502, Japan*

(*Received December 06, 2013, Revised June 13, 2014, Accepted July 28, 2014*)

Abstract. The steel-concrete composite decks have high fatigue durability and deformability in comparison with ordinary RC slabs. Withal, the steel-concrete composite deck is mostly heavier than the RC slabs. We have proposed herein a new type of steel-concrete composite deck which is lighter than the typical steel-concrete composite decks. This can be achieved by arranging hollow sectional members as shear connectors, namely, half-pipe or channel shear connectors. The present study aims to experimentally investigate mechanical characteristics of the half-pipe shear connectors under the direct shear force. The shear bond capacity and deformability of the half-pipe shear connectors are strongly affected by the thickness-to-diameter ratio. Additionally, the shear strengths of the hollow shear connectors (i.e., the half-pipe and the channel shear connectors) are compared. Furthermore, shear capacities of the hollow shear connectors equivalent to headed stud connectors are also discussed.

Keywords: steel-concrete composite deck; hollow shear connector; thickness-to-diameter ratio; web thickness-to-width ratio; shear bond capacity

1. Introduction

Recently in Japan, various types of steel-concrete composite decks (SCCDs in abbreviation) have been investigated to be applied to an abundance of superstructures such as highway bridges. In the SCCDs, a steel deck plate and RC slab work together compositely and supplement their weakness each other. Therefore, the SCCDs have high fatigue durability and deformability in comparison with ordinary RC slabs. The mechanical performance of SCCDs significantly depends on the arrangement of shear connectors. The headed stud connector is widely used. The headed stud is also applied to the profiled steel sheeting composite deck (Smith and Couchman 2010). The comparison of multi-stud and single stud is discussed by Xue (Xue *et al*. 2012). Mechanical behavior of channel's flange welded shear connectors is conducted by Maleki and Mahoutian (2009) and Baran and Topkaya (2012). Perfobond strips have been also used as shear connectors

∗Corresponding author, Associate Professor, E-mail: uenaka@kobe-kosen.ac.jp
[a] Associate Professor, E-mail: h-hirosi@civileng.kindai.ac.jp

http://www.techno-press.org/?journal=scs&subpage=8 ISSN: 1229-9367 (Print), 1598-6233 (Online)

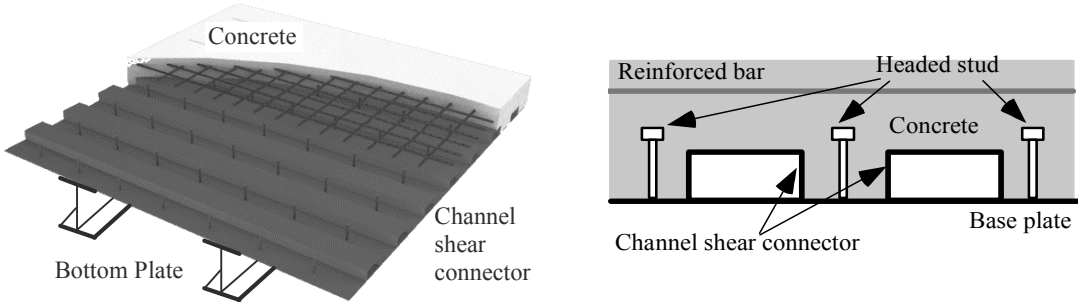

(a) Over view (b) Cross sectional view

Fig. 1 Steel-concrete composite deck welded with channel shear connectors (C-SCCD, Uenaka 2010)

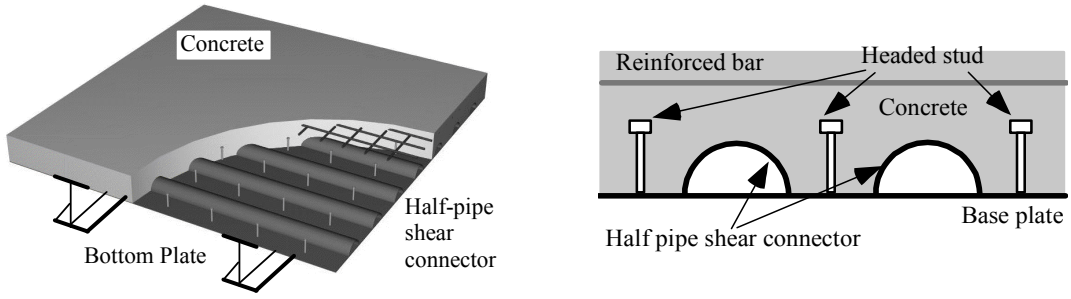

(a) Overview (b) Cross sectional view

Fig. 2 Steel-concrete composite deck welded half-pipe shear connectors (H-SCCD)

and their mechanical performance was investigated so far (Cândido-Martins *et al*. 2010, Ahn *et al*. 2010, Costa-Neves *et al*. 2013).

Having high fatigue durability and deformability, the SCCDs have been increasingly constructed for recent years in Japan. However, the SCCDs are generally heavier than ordinary RC slabs for superstructures. It can be expected to reduce self-weight of the SCCDs because the lighter SCCD will reduce dead load and seismic damage for substructures such as a pier.

Under the aforementioned background, the authors have proposed the lightweight SCCD consisting of the channel members welded on a bottom steel plate with headed studs and RC slab as shown in Fig. 1. The channel members as shear connectors with the hollow section inside can reduce self-weight of the SCCD, abbreviated as C-SCCD. We had experimentally conducted on the mechanical behavior of the channel shear connectors (CSCs in abbreviation) subjected to the direct shear force (Uenaka *et al*. 2010). Then, it was clear that the CSCs hold a good deformability and the shear bond capacity which are meaningfully affected by the channel web thickness-to-width ratio. Furthermore, the fatigue strength between the channel welded joint and the steel plate has been investigated by the authors (Higashiyama *et al*. 2010). It was found that the fatigue strength of welded joint was appropriate to the C grade of the Fatigue Design Recommendation specified in Japanese Society of Steel Construction.

In the following, we have also proposed a new type of SCCD consisting of RC slab and the half-pipe shear connectors (HPSCs in abbreviation) welded on a bottom steel plate with headed

stud connectors, H-SCCD, as shown in Fig. 2. Reduction of self-weight of the H-SCCD due to the hollow section inside the HPSCs can be anticipated. For the practical application of the HPSCs as the shear connectors in a SCCD, it is needed to verify the mechanical characteristics of HPSCs under the direct shear force.

This study aims to investigate the shear bond capacity of eight HPSCs through the push-out testing method. Main testing parameters selected were thickness (t) and diameter (D) of the HPSC. From the test results, a simple method to predict the shear bond capacity of the HPSC was proposed. Additionally, a comparison of shear strengths of the two hollow shear connectors (i.e. the HPSC and the CSC) was discussed including headed stud connectors. The part of this study has been reported previously. (Uenaka *et al*. 2009, Uenaka and Higashiyama 2013).

2. Proposed steel-concrete composite deck

The proposed H-SCCD in detail is shown in Figs. 2(a) and (b). The H-SCCD is composed of RC slab and the HPSCs welded on a bottom steel plate with headed stud connectors. Several headed stud connectors are arranged to withstand the transverse shear force. The HPSCs and the headed stud connectors also work together for the horizontal shear force which acts in the longitudinal direction. Moreover, the HPSCs welded on the bottom steel plate contribute to increasing rigidity of the bottom steel plate. The H-SCCD having the hollow section inside the HPSC is consequently lighter than typical SCCDs. Additionally, when hot or cold liquid runs through inside the hollow section, the internal temperature of SCCD may be warmed up or cooled down.

Table 1 Unit weight of SCCDs

Detailed deck	Robinson	Channel	Truss	C-SCCD	H-SCCD
Slab thickness (mm)	260	260	260	260	260
Thickness of bottom plate (mm)	8.0	6.0 or 8.0	6.0	6.0	6.0
Unit weight (kN/m^2)	7.00	7.40	7.08	6.20	6.08
Weight ratio	1.15	1.22	1.16	1.02	1.00

Table 2 List of HPSC specimens

No.	Tag.	Half pipe			Concrete
		Diameter	Thickness	Ratio	
		D (mm)	t (mm)	t / D	f_c' (N/mm^2)
1	D165-45	165	4.5	0.027	30.9
2	D165-50	165	5.0	0.030	30.9
3	D165-60	165	6.0	0.036	32.4
4	D140-23	140	2.3	0.016	30.2
5	D140-32	140	3.2	0.023	30.2
6	D140-40	140	4.0	0.029	28.4
7	D140-45	140	4.5	0.032	28.4
8	D140-60	140	6.0	0.043	28.4

Table 3 List of CSC specimens (Uenaka *et al*. 2010)

No.	Tag.	Height		Thickness		Ratio		f_c' (N/mm^2)
		Flange H (mm)	Web B_c (mm)	Web t_1	Flange t_2	H/B_c	t_1/B_c	
1	C125-65	125	65	6.0	8.0	0.52	0.092	19.5
2	C150-75-A	150	75	6.5	10.0	0.50	0.087	24.6
3	C150-75-B	150	75	9.0	12.5	0.50	0.120	24.6
4	C200-90	200	90	8.0	13.5	0.45	0.089	24.5
5	C100-50	100	50	5.0	7.50	0.50	0.100	27.2

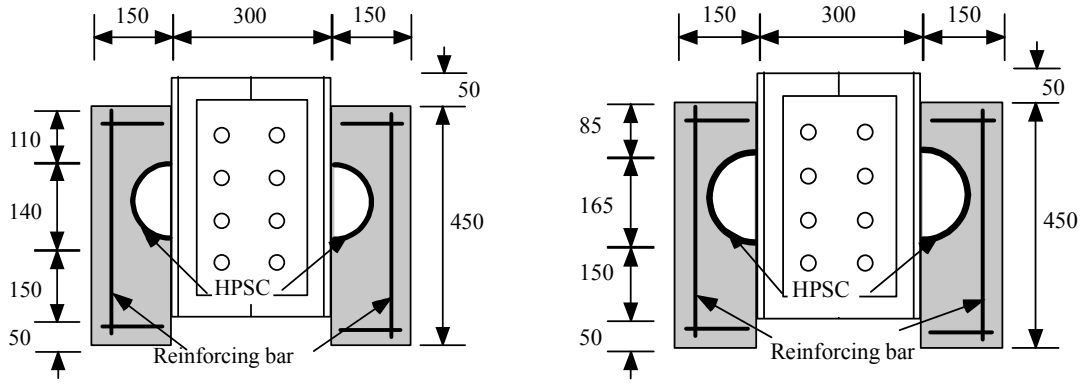

(a) Specimen with D = 140 mm (b) Specimen with D = 165 mm

Fig. 3 HPSC specimens for the push-out tests

Table 1 summarizes the comparison of unit weight of the H-SCCD and typical SCCDs including the C-SCCD being proposed previously. The SCCSs with channels or truss-shaped steel plates are composed of channels or truss-shaped steel plates welded on bottom steel plate and RC slab. The calculating results indicate that the H-SCCD is from 15 to 20% lighter than the typical SCCDs. Close to the self-weight, the C-SCCD approximately agrees with that of the H-SCCD.

3. Push-out tests

3.1 Test specimens

Fig. 3 and Table 2 show the details of HPSC specimens for push-out tests. Test specimens are manufactured based on Japanese Society of Steel Construction (JSSC 1996). The specimens are combinations of diameter and thickness of the HPSC as shown in Table 2. Details of the CSC specimens being conducted previously are also shown in Table 3. For all specimens, the RC slab has 150 mm in thickness, 300 mm in width, and 450 mm in height. Four deformed reinforcing bars with a diameter of 10 mm were placed to prevent unnecessary cracking of the concrete before reaching the ultimate load.

The nominal diameter of the HPSC was varied as 165 or 140 mm and thickness of that ranged from 2.3 to 6.0 mm. Therefore, the thickness-to-diameter ratio (t/D) ranged from 0.016 to 0.043. The tensile strength of the HPSC was 400 N/mm^2.

The friction between the flange of H-shaped steel member and the HPSC was eliminated by grease before concrete casting. The test specimen was placed on the abutment of loading machine with cement paste at the bottom of the RC slab in order to adjust unevenness as shown in Fig. 4 (JSSC 1996).

Direct shear force between the HPSC and the RC slab was applied through the H-shaped steel member by the universal loading machine as shown in Fig. 4.

3.2 Measurement

Two displacement transducers were arranged under the loading plate to measure the relative slip between the HPSC and the RC slab. Whereas, for two of the HPSC specimens, namely, D140-23 and D140-32, three axial strain gages were attached on the side surface of the RC slab beneath the HPSC to obtain the strain distributions as shown in Fig. 5.

4. Results and discussion

4.1 Failure modes

Two failure modes were observed in this study such as the concrete cracking and/or the compressive failure of the RC slab under the HPSC as shown in Figs. 6(a) and (b). In the specimen, D165-50, both the concrete cracking and the compressive failure of the RC slab under the HPSC can be observed as shown in Fig. 6(a). Furthermore, the D140-60 specimen exhibited the compressive failure near the welded joint of the HPSC without the concrete cracking as shown in

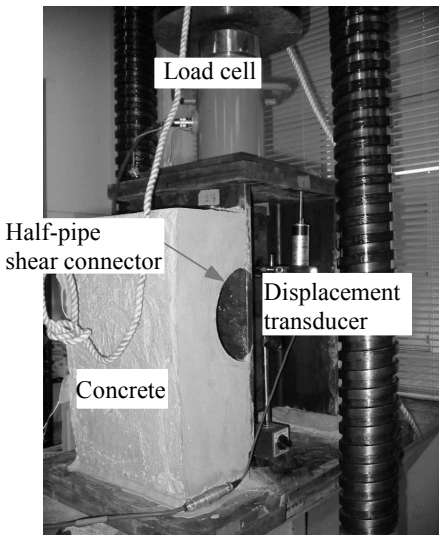

Fig. 4 Test setup (HPSC)

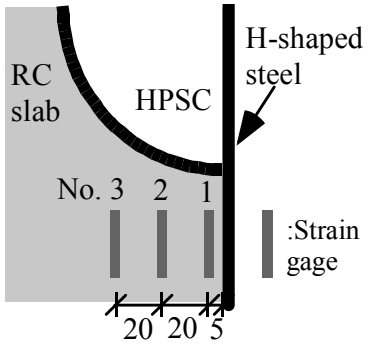

Fig. 5 Position of strain gages

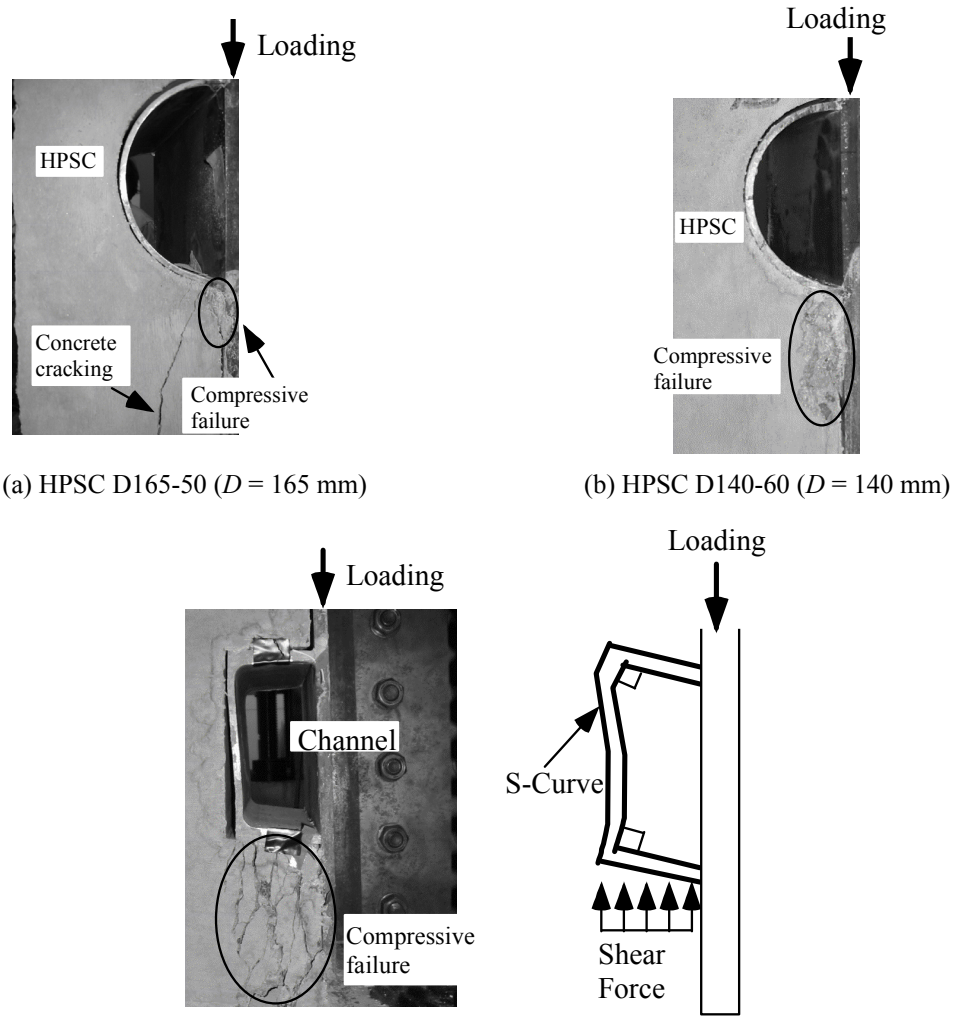

(a) HPSC D165-50 (D = 165 mm)

(b) HPSC D140-60 (D = 140 mm)

(c) CSC (Uenaka *et al*. 2010)

Fig. 6 Failure modes

Fig. 6(b). This is because the direct shear action concentrated around the welded joint of the HPSC. No cracking of a fillet welding of the HPSC was found.

Moreover, it can be also found that the compressive failure zone of D140-60 is larger than that of D165-50. This fact indicates that the bearing stress distribution under the HPSC can be assumed to be more uniform in D140-60. On the other hand, the bearing stress of D165-60 is concentrated close to the welded joint.

With respect to the CSC specimens tested in the previous study (Uenaka *et al*. 2010), the compressive failure of the RC slab under the CSC can be found as shown in Fig. 6(c). This fact indicates that the bearing stress distributed more uniformly under the CSC. As shown in Fig. 6(c), S-curve shaped deformation of the channel web was observed after the compressive failure of the RC slab under the CSC.

4.2 Shear force-slip curve

Figs. 7(a), (b) and (c) show the relationships between the shear force ($Q = P/2$, P: applied load) and the relative slip between the HPSC and the RC slab. In the specimens of D = 140 mm

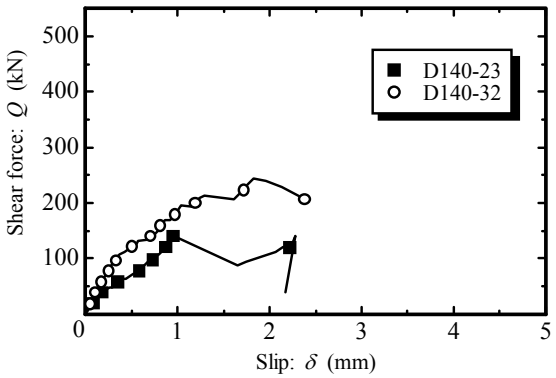

(a) HPSC (D140-23, D140-32)

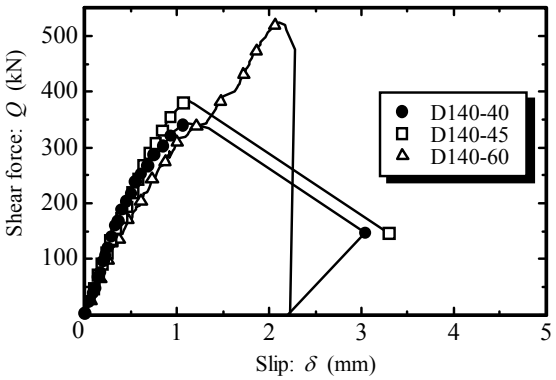

(b) HPSC (D140-40, D140-45, D140-60)

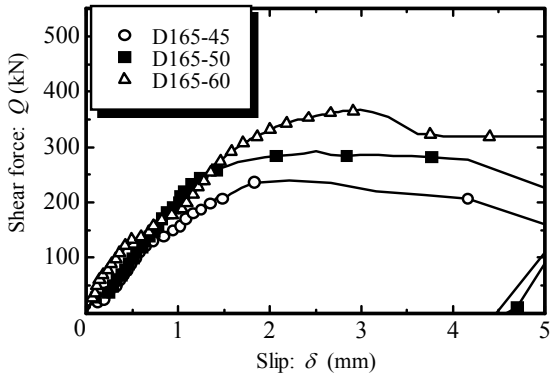

(c) HPSC (D = 165 mm)

Fig. 7 Shear force-slip curve

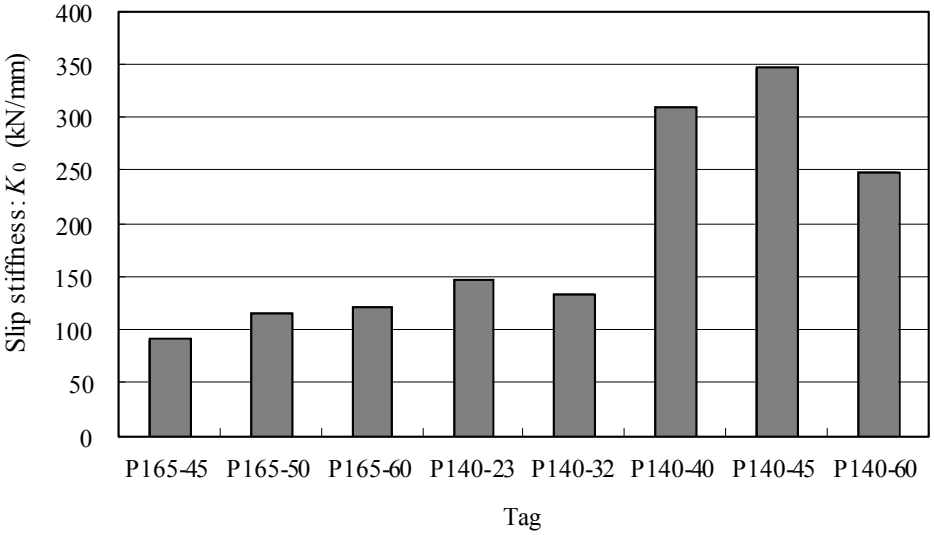

Fig. 8 Slip stiffness

with t/D being larger than 0.029 in Fig. 7(b), the deformation curves increase to be relatively linear up to the peak shear force. The peak shear force can be found within 2 mm slip. On the other hand, the deformation curves of the specimens with D = 165 mm in Fig. 7(c) draw flexible behavior as well as headed stud connectors. It can be also found that the deformability increases as t/D increases. Moreover, the peak shear force of D = 165 mm specimens appeared between 2 and 4 mm slip.

Additionally, Fig. 8 shows the slip stiffness, K_0 of all the specimens tested in this study. The slip stiffness K_0 is expressed as below,

$$K_0 = \frac{Q_u}{\delta_0} \tag{1}$$

where Q_u is the shear bond capacity (kN) and δ_0 is the slip (mm) when the shear bond capacity is obtained, respectively. The slip stiffness (K_0) of the specimen with flexible slip behavior is almost less than 150 kN/mm. It can be also found that the D140 specimen with t/D being less than 0.023 draws flexible behavior as same as D160 specimens.

Lastly, Figs. 9(a) and (b) show the relationships between the shear force and the relative slip of the CSCs which were previously reported (Uenaka *et al*. 2010). The shear force of all the specimens increased linearly up to the peak shear force. After the peak shear force, the shear force decreased abruptly owing to the compressive failure of the RC slab. This phenomenon is close to the behavior of the largest t/D of the HPSC, D140-60.

4.3 Shear bond capacity

4.3.1 Half-pipe shear connector (HPSC)

Fig. 10 shows the relationship between the gages' position shown in Fig. 5 divided by the HPSC's diameter ($D/2$) and the concrete strain measured on the RC slab's surface. The tensile

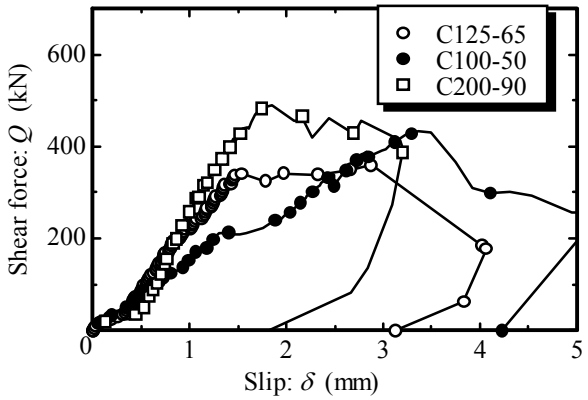

(a) H = 100, 125 and 200 mm specimens

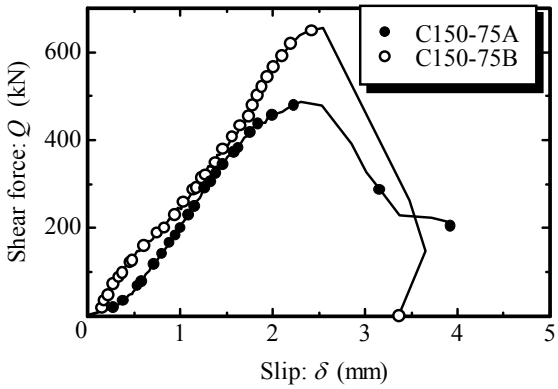

(b) H = 150 mm specimens

Fig. 9 Shear force-slip curve of CSC (Uenaka *et al*. 2010)

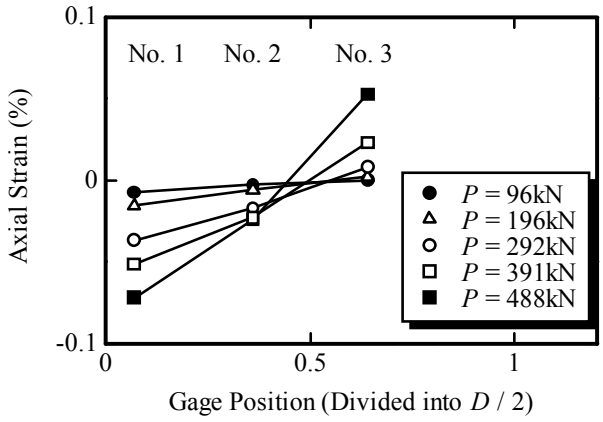

Fig. 10 Strain distribution (D140-32)

strain is taken as positive. Although the strains at No. 1 and No. 2 positions exhibited in compressive, the stain at No. 3 position increased toward in tension with increasing the applied load. This fact indicates that the local bending moment occurred in the HPSC.

The shear bond capacities (Q_u) of the HPSCs and the CSCs are summarized in Tables 4(a) and (b), respectively. Herein, the shear strength can be calculated as the following equation assumed to be triangular stress distribution such as in Fig. 10,

$$\tau_u = \frac{4Q_u}{rB} \tag{2}$$

where τ_u is the shear bond strength (N/mm^2), r is the diameter of the HPSC (140 or 165 mm), and B is the width of the HPSC (= 300 mm).

Furthermore, the relationship between the normalized shear strength (τ_u / f_c') and the thickness-to-diameter ratio (t / D) is shown in Fig. 11. From Fig. 11, the relationship between the normalized shear strength τ_u / f_c') and t / D can be found almost linearly. The normalized shear strength is meaningfully affected by t / D. The method of least squares being applied, the normalized shear strength of the HPSC under the parameter of t / D ranging from 0.02 to 0.04 can be expressed as below.

$$\frac{\tau_u}{f_c'} = 78.2\frac{t}{D} \quad \text{(for } D140 \text{ series of specimens)} \tag{3a}$$

$$\frac{\tau_u}{f_c'} = 49.2\frac{t}{D} \quad \text{(for } D165 \text{ series of specimens)} \tag{3b}$$

Table 4 Test results

(a) HPSC

No.	Tag	P_u (kN)	Q_u (kN)
1	D165-45	480.2	240.1
2	D165-50	585.1	292.5
3	D165-60	733.0	366.5
4	D140-23	280.3	140.1
5	D140-32	488.0	244.0
6	D140-40	688.9	344.5
7	D140-45	772.2	386.1
8	D140-60	1047.6	523.8

(b) CSC (Uenaka *et al*. 2010)

No.	Tag	P_u (kN)	Q_u (kN)
1	C125-65	718.3	359.2
2	C150-75-A	973.1	486.6
3	C150-75-B	1308.3	654.2
4	C200-90	980.0	490.0
5	C100-50	865.3	432.7

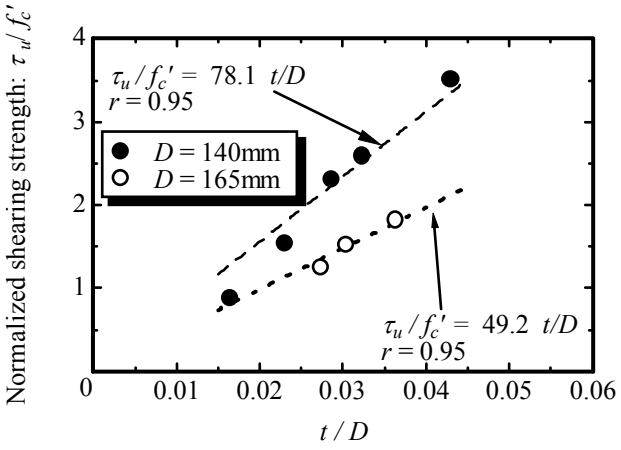

Fig. 11 Normalized shear strength and t/D

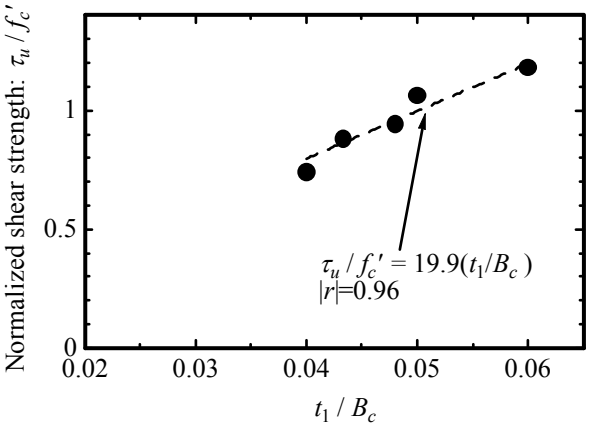

Fig. 12 Normalized shear strength and t_1 / B_c (Uenaka *et al*. 2010)

Therefore, the simply estimated shear bond capacity $Q_{u\text{-}est}$ of the HPSC can be proposed as below.

$$Q_{u-est} = \frac{f_c'}{4} rB\left(78.2\frac{t}{D}\right) \quad \text{(for } D140 \text{ series of specimens)} \tag{4a}$$

$$Q_{u-est} = \frac{f_c'}{4} rB\left(49.2\frac{t}{D}\right) \quad \text{(for } D165 \text{ series of specimens)} \tag{4b}$$

The difference of coefficients in Eqs. (3a) and (3b) is mainly due to the failure modes such as the compressive failure area and the concrete cracking of the RC slab beneath the HPSC as shown in Fig. 6. It can be also found that the D140 specimen with t/D being less than 0.023 can be predicted by Eq. (4a) being the dotted line as shown in Fig. 12. This is because these specimens exhibited flexible slip behavior as same as D160 specimen, namely, the slip stiffness K_0 is less

than 150 kN/mm. It can be also noted that Eqs. (3) and (4) are effective for f_c' ranging from 20 to 30 (N/mm^2).

4.3.2 Comparison of the HPSCs and the CSCs

According to Section 4.1, as the constant bearing stress distributed under the CSCs (Uenaka 2010), the shear strength (τ_u) can be simply expressed as below,

$$\tau_u = \frac{Q_u}{Hw} \tag{5}$$

where Q_u is the shear bond capacity (N), H and w are the height and the width of the CSC (= 300 mm), respectively. The shear bond capacities of the CSCs are also summarized in Table 4(b).

The normalized shear strength for the CSCs had been proposed in the previous study (Uenaka *et al*. 2010), namely,

$$\frac{\tau_u}{f_c'} = 19.9\frac{t_1}{B_c} \tag{6}$$

where t_1 and B_c are the web thickness and the web width of channel (mm), respectively.

The relationship between τ_u / f_c' and t_1 / B_c is shown in Fig. 12. It can be also noted that the estimation is appropriate for t_1/B ranging from 0.04 to 0.06. From Figs. 11 and 12, it can be found that the normalized shear strengths τ_u / f_c' for the HPSCs and the CSCs are affected by the ratio of the thickness (t or t_1) and the diameter or the height (D or B_c).

Table 5 Equivalent studs' number

(a) HPSC

No.	Tag	D16	D19	D22
1	D165-45	9.3	6.6	4.9
2	D165-50	10.3	7.3	5.5
3	D165-60	13.0	9.2	6.9
4	D140-23	7.4	5.2	3.9
5	D140-32	10.3	7.3	5.4
6	D140-40	12.1	8.6	6.4
7	D140-45	13.6	9.6	7.2
8	D140-60	18.1	12.8	9.6

(b) CSC (Uenaka *et al*. 2010)

No.	Tag	D16	D19	D22
1	C125-65	19.1	13.6	10.1
2	C150-75-A	19.9	14.1	10.5
3	C150-75-B	27.6	19.6	14.6
4	C200-90	22.1	15.7	11.7
5	C100-50	15.3	10.9	8.1

4.4 Comparison with the shear strength of headed stud connectors

Shear capacity of a headed stud connector (Q_u) is expressed as below,

$$Q_u = 0.5 A_s \sqrt{E_c f_c'} \tag{7}$$

where A_s is the cross sectional area of a headed stud connector (mm^2), E_c is the young's modulus of concrete (N/mm^2), and f_c' is the compressive strength of concrete (N/mm^2).

Equivalent number of headed stud connectors against the HPSC and the CSC can be calculated from Eqs. (4) and (7) or Eqs. (6) and (7). The total cross sectional area can be expressed as Eqs. (8) and (9), namely,

$$A_s = 24.6 \sqrt{\frac{f_c'}{E_c}} rB \cdot \frac{t}{D} \quad (\text{for } D = 160 \text{ mm of the HPSCs}) \tag{8a}$$

$$A_s = 39.1 \sqrt{\frac{f_c'}{E_c}} rB \cdot \frac{t}{D} \quad (\text{for } D = 140 \text{ mm of the HPSCs}) \tag{8b}$$

$$A_s = 39.8 \sqrt{\frac{f_c'}{E_c}} Hw \cdot \frac{t_1}{B_c} \quad (\text{for the CSCs}) \tag{9}$$

Table 5 summarizes the equivalent number of headed stud connectors for unit length. For example, it can be found that the shear strength of D165-60 is equivalent to thirteen headed stud connectors with a diameter of 16 mm.

5. Conclusions

The steel-concrete composite deck having the hollow sectional shear connectors welded on a bottom steel plate has been proposed. Under the parameter such as the thickness-to-diameter ratio of the HPSC, the mechanical behavior of the HPSC subjected to the direct shear force was mainly discussed including the test results of the CSCs carried out in the previous study. From the test results, the following remarks can be drawn:

- Observed failure modes were the concrete cracking and the compressive failure beneath the HPSC. In the specimen of D165-50, the failure mode observed was both the concrete cracking and the compressive failure of the RC slab under the welded joint of the HPSC. The compressive failure zone of D140 series of specimens was larger than that of D165 series of specimens. This is due to the deformability of the HPSC. On the contrary, the observed failure mode of the CSCs was the compressive failure of RC slab under the CSC with S-curve shaped deformation of the channel web.
- In the D140 specimens, the shear force reached to the maximum value within 2 mm slip. On the other hand, in the D165 specimens, the specimens deformed flexibly rather than the D140 specimens and the maximum shear force was obtained between 2 and 4 mm slip.
- The slip stiffness of the D140 specimens with t/D being less than 0.023 exhibited flexible behavior as same as the D165 specimens.

- The shear bond capacity (Q_u) of the HPSCs increased as t/D increased. This is because the local bending moment gradually increased as the HPSC's thickness increased. A simple method to predict the shear bond capacity of the HPSC subjected to the direct shear force was proposed with respect to t/D considering the triangular stress distribution in the RC slab under the HPSC.
- We proposed a calculation method to estimate the hollow shear connectors of shear capacities equivalent to headed stud connectors.

Acknowledgments

The authors thank Mr. M. Shimizu and Mr. R. Okamoto, formerly as advance course students of Kobe City College of Technology (KCCT), for their experimental assistance. We also thank Dr. T. Ishikawa, who is an assistant professor in Kyoto University, for the sincere help to this study.

References

Ahn, J.H., Lee, C.G., Won, J.H. and Kim, S.H. (2010), "Shear resistance of the perfobond-rib shear connector depending on concrete strength and rib arrangement", *J. Construct. Steel Res.*, **66**(10), 1295-1307.

Baran, E. and Topkaya, C. (2012), "An experimental study on channel type shear connectors", *J. Construct. Steel Res.*, **74**, 108-117.

Cândido-Martins, J.P.S., Costa-Neves, L.F. and Vellasco, P.C.G. da S. (2010), "Experimental evaluation of the structural response of Perfobond shear connectors", *Eng. Struct.*, **32**(8), 1976-1985.

Costa-Neves, L.F., Figueiredo, J.P., Vellasco, P.C.G. da S. and Vianna, J. da C. (2013), "Perforated Shear Connectors on Composite Girders under Monotonic Loading: An Experimental Approach", *Eng. Struct.*, **56**, 721-737.

Higashiyama, H., Ishikawa, T. and Uenaka, K. (2010), "Fatigue strength of welded joint between channel shape steel and steel plate in steel and concrete composite deck", *Proceedings of the 5th Civil Engineering Conference in the Asian Region and Australasian Structural Engineering Conference 2010*, Sydney, Australia, August, Paper No. 331.

Japanese Society of Steel Construction (1996), Research report on push out test method on headed stud connector and its current research, JSSC Technical Report. [In Japanese]

Maleki, S. and Mahoutian, M. (2009), "Experimental and analytical study on channel shear connectors in fiber-reinforced concrete", *J. Construct. Steel Res.*, **65**(8-9), 1787-1793.

Smith, A.L. and Couchman, G.H. (2010), "Strength and ductility of headed stud shear connectors in profiled steel sheeting", *J. Construct. Steel Res.*, **66**(6), 748-754.

Uenaka, K. and Higashiyama, H. (2013), "Experimental study on half-pipe shear connectors under direct shear", *Proceedings of the 2013 World Congress on Advances in Structural Engineering and Mechanics* (*ASEM'13*), Jeju, Korea, September, pp. 2111-2119.

Uenaka, K., Higashiyama, H., Ishikawa, T. and Okamoto, R. (2009), "Push-out test on half-pipe shear connector", *Proceedings of the Japan Concrete Institute*, **31**(2), 1117-1122. [In Japanese]

Uenaka, K., Higashiyama, H. and Ishikawa, T. (2010), "Mechanical behavior of channel shear connector under direct shear", *Proceedings of the 5th Civil Engineering Conference in the Asian Region and Australasian Structural Engineering Conference 2010*, Sydney, Australia, August, Paper No. 117.

Xue, D., Liu, Y., Yu, Z. and He, J. (2012), "Static behavior of multi-stud shear connectors for steel-concrete composite bridge", *J. Construct. Steel Res.*, **74**, 1-7.

CC